RSC Advances

PAPER

View Article Online
View Journal | View Issue

Cite this: *RSC Adv.*, 2022, **12**, 16589

I_2/TBHP mediated domino synthesis of 2-(2,4-dioxo-1,4-dihydroquinazolin-3(2*H*)-yl)-*N*-aryl/alkyl benzamides and evaluation of their anticancer and docking studies†

Anil Kumar Soda,[ab] Phani Krishna C. S,[a] Sai Krishna Chilaka,[ab] Vamshi Krishna E,[bc] Sunil Misra [bc] and Sridhar Madabhushi *[ab]

Received 5th April 2022
Accepted 24th May 2022

DOI: 10.1039/d2ra02216h

rsc.li/rsc-advances

A novel I_2/TBHP mediated domino synthesis of 2-(2,4-dioxo-1,4-dihydroquinazolin-3(2*H*)-yl)-*N*-phenyl benzamides by reaction of isatins with *o*-amino *N*-aryl/alkyl benzamides was described. This was the first application of *o*-amino *N*-aryl/alkyl benzamides participating in oxidative rearrangement with isatins for synthesis of desired products. The synthesized compounds contained amide and quinazoline units and their combination resulted in molecular hybridization of two important pharmacophores. In this study, the synthesized compounds **3a–r** were screened for cytotoxicity against four cancer cell lines A549, DU145, B16-F10, and HepG2 and also non-cancerous cell line CHO-K1. The compounds **3c**, **3l** and **3o** gave promising results. The *in silico* molecular docking studies (PDB ID 1N37) also validated the anticancer activity of these compounds showing good binding affinity with target DNA and by acting as DNA intercalators.

Introduction

Molecular hybridization has been a strategy in drug discovery research in recent years.[1] It involves blending or linking of two or more pharmacophore moieties to generate a single molecular entity which could exhibit better selectivity, and improved affinity and activity, and overcome the drug resistance due to a mixed mechanism of action. Cancer, a debilitating disease, is a worldwide major human health problem. Though many anticancer agents are available, still there is a call to identify effective and safe drugs for treatment of cancer. Numerous heterocyclic compounds have been researched to discover new anticancer agents.[2]

Quinazoline pharmacophore is found in various pharmaceuticals including antimicrobials and cytotoxic agents.[3–5] Quinazolines exhibit a wide range of biological properties such as anti-hypertensive,[6] anti-HIV-1,[7] anti-cancer,[8] antitumor,[9] anti-inflammatory,[10] progesterone receptor antagonists[11] and antibacterial activity.[12] Some small molecules containing quinazolines motif are also known to exhibit potent and specific puromycin-sensitive amino peptidase (PSA) inhibitory activity[13] and reversible inhibition of Bruton's tyrosine kinase (BTK).[14] Quinazoline scaffold is found also in several natural products.[15]

Carboxamide scaffolds are of immense interest in medicinal chemistry.[16,17] The pharmaceutically important ergot alkaloids such as dehydro ergotamine and ergotamine contain amide linkage. There are many drugs like atorvastatin, valsartan, paracetamol and penicillin available in the market, which contains amide linkage in the nucleus and possesses varied therapeutic activities like antimycobaterial, antimicrobial, antifungal, cytotoxic, antiepileptic and analgesic properties.[2,18] The amide bond is planar, resonating and stable with large dipole moment, resembles the protein's peptide linkage.[19] Use of peptide-based therapeutics is steadily increasing, for example, cyclosporine A is a peptide which is a widely used powerful immunosuppressive agent.[20] Anticancer agents with amide pharmacophore[21] and quinazoline pharmacophore are shown in Fig. 1.

Hybrid drugs with multiple mechanism of action are of great interest for cancer treatment, for example, quinazoline-amide hybrid drug raltitrexed[1c] known for potent anticancer activity.[22] In the present work, we aimed at synthesis of 2-(2,4-dioxo-1,4-dihydroquinazolin-3(2*H*)-yl)-*N*-aryl/alkyl benzamides, which were new quinazoline-amide hybrid molecules. No literature is available for synthesis of these quinazoline-amide hybrid molecules. Some existing literature was available for synthesis of simple 2,4-quninozolinediones[23] but these methods had one or more disadvantages such as metal catalysts, harsh reaction conditions and limited substrate scope.

[a]*Fluoro-Agrochemicals Department, CSIR-Indian Institute of Chemical Technology, Hyderabad-500007, India. E-mail: sridharm@iict.res.in*

[b]*Academy of Scientific and Innovative Research (AcSIR), Ghaziabad-201002, India*

[c]*Applied Biology Division, CSIR-Indian Institute of Chemical Technology, Hyderabad-500007, India*

† Electronic supplementary information (ESI) available. See https://doi.org/10.1039/d2ra02216h

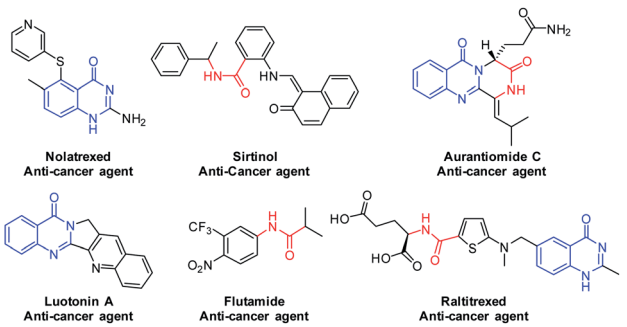

Fig. 1 Cancer drugs with quinazoline, amide and hybrid pharmacophores.

Under existing literature conditions were not promoted the synthesis of desired molecular hybrids 2-(2,4-dioxo-1,4-dihydroquinazolin-3(2*H*)-yl)-*N*-aryl/alkyl benzamides by reaction of isatins with 2-amino-(*N*-alkly/aryl) benzamides. Therefore, we were much interest to synthesize these quinazoline-amide hybrid molecules, because of their important applications in organic synthesis and medicinal chemistry. Moreover, I_2/TBHP mediated oxidative coupling reactions are very important than those transition-metal-mediated oxidative reactions for they are greener and less expensive. It has been widely studied and applied for a variety of oxidation reactions.[24]

Domino reactions have been one of the mainly constructive and powerful synthetic tools in organic synthesis. The advantage of these domino reactions as a methodology involve two or more bond constructions that takes place under the same reaction conditions in one-pot. In the past several years, authors have developed a variety of multicomponent domino reactions that can afford easy access to functionalized various heterocycles.[25]

Here, we observed for the first time a new domino reaction of isatins with 2-amino *N*-aryl/alkyl benzamides in the presence of I_2/TBHP under reflux in methanol to give 2-(2,4-dioxo-1,4-dihydroquinazolin-3(2*H*)-yl)-*N*-aryl/alkyl benzamides in high yields with broad functional group tolerance and short reaction time as shown in Scheme 1.

To the best of our knowledge, this I_2/TBHP reagent system has not been used for preparation of 2-(2,4-dioxo-1,4-dihydroquinazolin-3(2*H*)-yl)-*N*-aryl/alkyl benzamides through oxidative rearrangement of isatins and 2-amino-(*N*-alkly/aryl) benzamides.

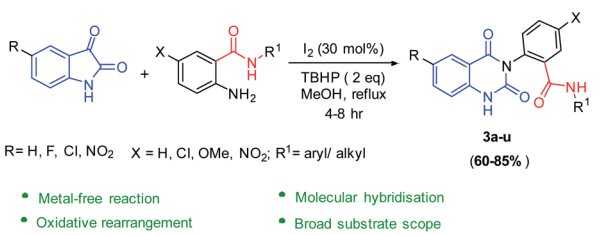

Scheme 1 Synthesis of 2-(2,4-dioxo-1,4-dihydroquinazolin-3(2*H*)-yl)-*N*-aryl/alkyl benzamides.

Furthermore, all the synthesized compounds were well characterized and assessed for their cytotoxicity by MTT assay against four cancer cell lines such as A549, DU145, B16-F10, HepG2 and non-cancerous cell line CHO-K1. In addition, to understand the structure–activity relationships, evaluate the possible intercalating potency of the synthesized compounds with DNA and validate the biological studies, molecular docking studies were conducted.

Results and discussion

Chemistry

In our preliminary experiments, reaction of isatin **1a** with 2-amino-*N*-phenylbenzamide **2a** in presence of *t*-butyl hydroperoxide (TBHP, 2 equivalents) as oxidant and iodine as a catalyst (10 mol%) under reflux in methanol gave 2-(2,4-dioxo-1,2-dihydroquinazolin-3(4*H*)-yl)-*N*-phenylbenzamide **3a** in 70% yield (entry 1, Table 1). In this reaction, yield of **3a** was found to increase with increasing amount of catalyst, for example, 20% and 30 mol% of iodine gave **3a** in 80% and 85% yields respectively (entries 2 and 3, Table 1). In the absence of I_2/TBHP, no reaction was observed (entry 4, Table 1). These observations showed that catalyst played important role in the formation of product **3a**. We also studied the reaction using 30 mol% of iodine and H_2O_2 as oxidant to obtain **3a** in 65% yield (entry 5, Table 1). We also studied the action using 30 mol% of iodine and TBHP in various solvents such as acetonitrile, ethanol, 2-propanol, 1,2-dichloroethane (DCE), dichloromethane, toluene, 1,4-dioxane and chloroform to obtain **3a** in 80%, 78%, 76%, 73%, 72%, 70%, 60% and 50% yields respectively (entries 6–13, Table 1). In the absence of solvent, no reaction was observed (entry 14, Table 1).

Table 1 Optimization of reaction conditions

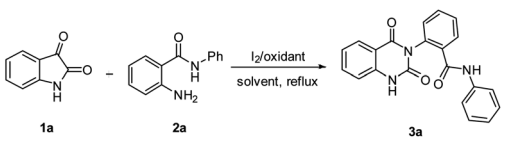

Entry	I_2 (mol%)	Oxidant (2 eq.)	Solvent	Time (h)	% Yield[a] (**3a**)
1	I_2 (10)	TBHP	MeOH	15	70
2	I_2 (20)	TBHP	MeOH	15	80
3	I_2 (30)	TBHP	MeOH	4	85
4	—	—	MeOH	15	NR
5	I_2 (30)	H_2O_2	MeOH	15	65
6	I_2 (30)	TBHP	CH_3CN	15	80
7	I_2 (30)	TBHP	EtOH	15	78
8	I_2 (30)	TBHP	2-Propanal	15	76
9	I_2 (30)	TBHP	DCE	15	73
10	I_2 (30)	TBHP	DCM	15	72
11	I_2 (30)	TBHP	Toulene	15	70
12	I_2 (30)	TBHP	1,4-Dioxane	15	60
13	I_2 (30)	TBHP	CH_3Cl	15	50
14	I_2 (30)	TBHP	—	15	NR

[a] Isolated yields. NR = no reaction.

Table 2 Scope of 2-aminobenzamides

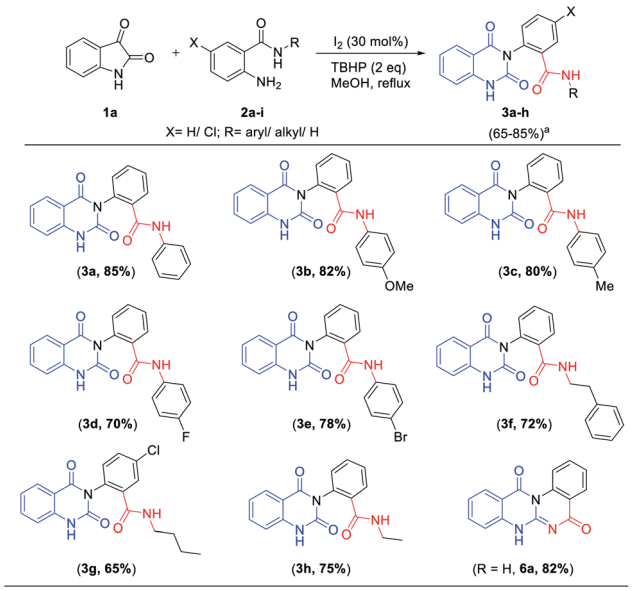

[a] Isolated yields. All products gave satisfactory ^{1}H NMR, ^{13}C NMR, IR and mass spectral data.

After the condition was optimal (entry 3, Table 1), we next turned our interest towards evaluating the generality of this transformation with different 2-amino-(*N*-alkyl/aryl) benzamides (**2a–h**), which contain phenyl, methoxy, methyl, fluoro, bromo, phenethyl, *n*-butyl or ethyl group on the aryl ring and *N*-alkyl or *N*-aryl functionality on the amide group. These compounds afforded 2-(2,4-dioxo-1,4-dihydroquinazolin-3(2*H*)-yl)-*N*-aryl/alkyl benzamides **3a–h** (Table 2) in good to excellent yields (65–85%). Interestingly, having free amide functionality the corresponding quinazolinedione product could undergo further cyclization to obtain 5*H*-quinazolino [3,2-*a*]quinazoline-5,12(7*H*)-dione **6a** in 82% yield as shown in Table 2. In this study, substituted 2-amino-(*N*-alkyl/aryl)benzamides with both electron donating and electron-withdrawing groups on amide group operate well in this transformation to produce the corresponding 2-(2,4-dioxo-1,4-dihydroquinazolin-3(2*H*)-yl)-*N*-aryl/alkyl benzamides in good to excellent yields.

Table 3 Scope of 2-amino (*N*-aryl/alkyl)benzamides and isatins

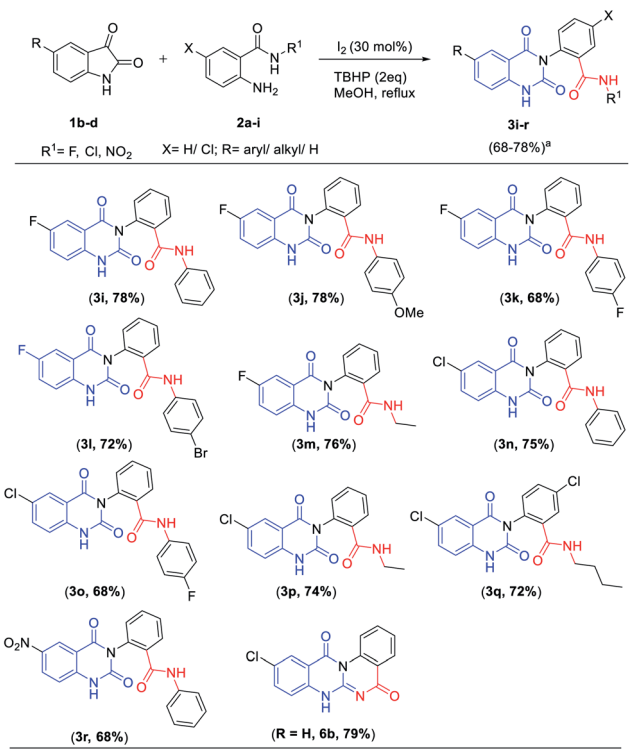

[a] Isolated yields. All products gave satisfactory ^{1}H NMR, ^{13}C NMR, IR and mass spectral data.

Table 4 Scope of 2-amino *N*-phenyl benzamides

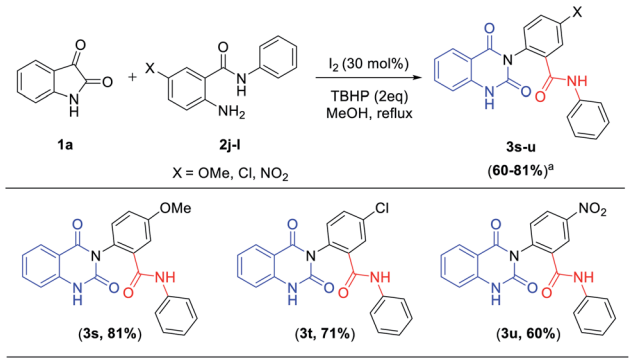

[a] Isolated yields.

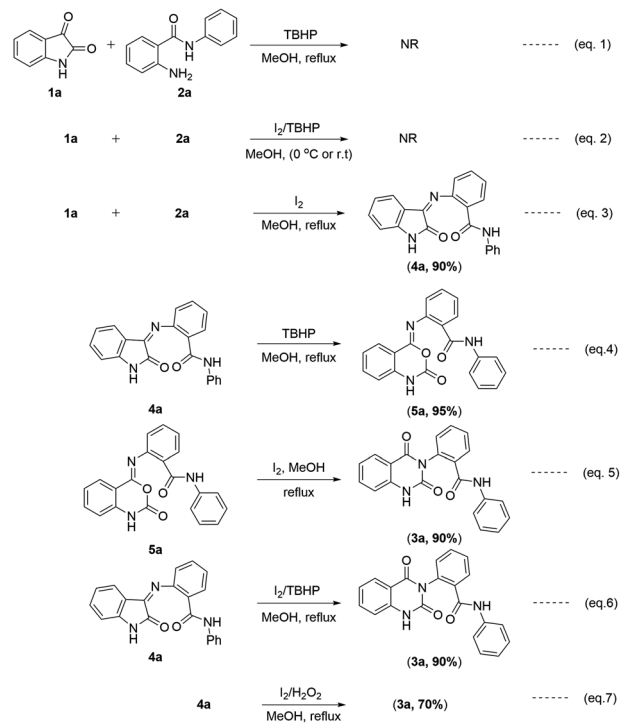

Scheme 2 Study of control experiments.

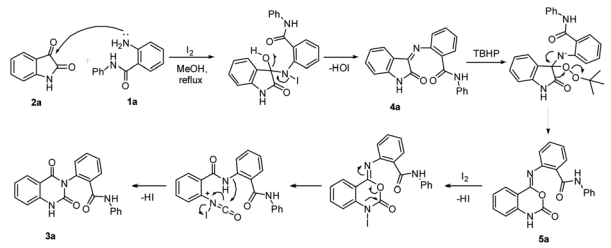

Scheme 3 Plausible mechanism for the formation of 2-(2,4-dioxo-1,2-dihydroquinazolin-3(4*H*)-yl)-*N*-phenylbenzamide (**3a**).

To further expand the substrate scope, the reactivity of diversely substituted isatins (**1b–d**) and 2-amino-(*N*-alkyl/aryl) benzamides (**2a–i**) were examined under optimized conditions (Table 3). Reactions of substituted isatins such as 5-fluoro-, 5-chloro-, 5-nitro isatins (**2b–d**) smoothly reacted with 2-amino (*N*-aryl/alkyl) benzamides containing 4-methoxy, 4-fluoro, 4-bromo, *n*-butyl and ethyl gave good to excellent yields (68–78%) and 2-amino *N*-phenylbenzamide **2i** react with 5-chloro isatin **1c** to produce the corresponding product **6b** in good yield of 79%.

To further expand the substrate scope, the reactivity of diversely substituted isatin (**1a**) and 2-amino-*N*-phenyl benzamides (**2j–l**) were examined under optimized conditions. Reactions of 5-OMe/5-chloro/5-nitro substituted 2-amino *N*-phenyl benzamides smoothly reacted with isatin gave quinazolinediones **3s–u** (Table 4) as good to excellent yields (60–81%). In this transformation isatin react with electron withdrawing group (–NO_2) contained 2-amino *N*-phenyl benzamide gave moderate yield (**3u**, 60%) when compared to electron donating group (–OMe) contained 2-amino *N*-phenyl benzamides (**3s**, 81%).

The results observed in the control experiments are shown in Scheme 2. In this study, formation of **3a** was observed only when reaction was conducted using I_2/TBHP under reflux in methanol. This reaction did not proceed when TBHP used alone, and also no reaction was observed when conduct at cooling and ambient temperatures (Scheme 2, eqn (1) and (2)). However, when the reaction was carried out in presence of iodine without oxidant, it gave the intermediate (*Z*)-2-((2-oxoindolin-3-ylidene)amino)-*N*-phenyl benzamide **4a** (Scheme 2, eqn (3)). In our study, the intermediate **4a** was found to react with TBHP and converted into intermediate (*Z*)-2-((2-oxo-1,2-dihydro-4*H*-benzo[*d*][1,3]oxazin-4-ylidene)amino)-*N*-phenylbenzamide **5a** (Scheme 2, eqn (4)). The important observation noted in this study is, the intermediate **5a** was converted into product **3a** when treated with iodine under reflux in methanol (Scheme 2, eqn (5)). The intermediate **4a** also directly converted into **3a** when treated with I_2/TBHP or I_2/H_2O_2 under reflux in methanol (Scheme 2, eqn (6) and (7)).

In view of the observations described above, the plausible reaction mechanism for the domino reaction of isatin **1a** and 2-amino-*N*-phenyl benzamide **2a** in the presence of I_2/TBHP is shown in Scheme 3. Here, the compound **4a** is initially produced by the condensation of isatin **1a** and 2-amino *N*-phenyl benzamide **2a** under catalysis of iodine. Next **4a**

Table 5 *In vitro* cytotoxicity of 2-(2,4-dioxo-1,4-dihydroquinazolin-3(2*H*)-yl)-*N*-aryl/alkyl benzamides derivatives against A549, B16-F10, DU145, HepG2 and CHO-K1 cell lines[a]

		IC_{50} values (μM)				
Sr. no.	Compounds	A549	B16-F10	DU145	HEPG2	CHO
1	**3a**	29.40 ± 0.45	39.51 ± 0.13	14.83 ± 0.13	8.73 ± 0.02	NA
2	**3b**	19.47 ± 0.25	24.78 ± 0.70	11.56 ± 0.06	23.30 ± 0.52	NA
3	**3c**	15.15 ± 0.70	17.90 ± 0.17	11.49 ± 0.04	5.33 ± 0.12	NA
4	**3d**	21.02 ± 0.12	25.77 ± 0.13	12.84 ± 0.01	14.19 ± 0.13	NA
5	**3e**	11.65 ± 0.14	14.67 ± 0.05	12.05 ± 0.02	9.48 ± 0.05	69.41 ± 5.17
6	**3f**	16.44 ± 0.53	43.95 ± 0.26	11.06 ± 0.34	14.39 ± 0.02	NA
7	**3g**	30.41 ± 5.52	20.51 ± 0.91	18.65 ± 0.08	15.30 ± 0.78	NA
8	**3h**	34.76 ± 4.65	27.14 ± 0.68	10.44 ± 0.02	16.71 ± 1.72	94.21 ± 2.44
10	**3i**	19.32 ± ±0.09	32.41 ± 0.13	11.47 ± 0.19	10.09 ± 0.07	83.21 ± 1.32
11	**3j**	30.38 ± 1.35	34.34 ± 1.55	12.33 ± 0.17	8.74 ± 0.34	NA
12	**3k**	17.17 ± 0.41	29.99 ± 0.42	11.59 ± 0.06	28.68 ± 0.92	NA
13	**3l**	17.42 ± 0.18	28.47 ± 0.31	12.63 ± 0.08	7.77 ± 0.02	51.54 ± 2.74
14	**3m**	26.27 ± 1.32	41.42 ± 0.81	19.39 ± 0.14	20.18 ± 0.31	88.04 ± 3.56
15	**3n**	14.69 ± 0.18	14.83 ± 0.01	10.43 ± 0.13	12.30 ± 0.26	73.88 ± 2.81
16	**3o**	26.32 ± 1.03	16.03 ± 0.06	5.17 ± 0.07	3.02 ± 0.06	74.53 ± 9.44
17	**3p**	22.75 ± 0.71	31.67 ± 0.14	13.02 ± 0.03	33.88 ± 0.71	NA
18	**3q**	28.67 ± 1.38	36.46 ± 0.10	9.37 ± 0.03	8.51 ± 0.20	NA
19	**3r**	16.70 ± 0.30	33.13 ± 0.12	15.59 ± 0.07	15.95 ± 0.51	NA
19	**4a**	23.76 ± 0.12	22.17 ± 0.56	17.37 ± 0.32	16.04 ± 0.41	NA
20	**5FU**	29.64 ± 1.64	7.55 ± 0.01	16.32 ± 0.02	22.97 ± 0.27	NA
Doxorubicin		0.55 ± 0.16	0.7 ± 0.56	0.363 ± 0.01	0.72 ± 0.012	8.8.1 ± 1.04

[a] A549 – *Homo sapiens* lung carcinoma (ATCC® CCL-185™); B16-F10 – *Mus musculus* mouse skin melanoma (ATCC® CRL-6475™); DU145 – *Homo sapiens* prostrate carcinoma (ATCC® HTB-81™); Hep G2 – *Homo sapiens* hepatocellular carcinoma (ATCC® HB-8065™); CHO-K1 – *Cricetulus griseus* chinese hamster ovary cells (ATCC® CCL-61™); **5FU**, 5-flourouracil, positive control, doxorubicin as standard drug-for comparison, NA – no activity.

Table 6 Molecular docking studies on DNA (PBD ID 1N37)

Compounds	Binding energy (kcal mol^{-1})	Inhibition constant (K_i)	H-bonds		π–π stacking	
			Nucleotides	Interacting atoms	Nucleotides	Interacting atoms
3c	−9.13	0.20 μM	DG A:5	Quinazoline ketone	DG B:13, DG A:5, DC B:12, DC A:4	C=C in amide aromatic ring
3l	−8.31	0.81 μM	DG A:5	Quinazoline ketone	DG B: 13, DG A: 5, DC B: 12, DC A: 4	C=C in amide aromatic ring
3o	−8.04	1.28 μM	DG B:13 DG A:5	Quinazoline ketone Amide ketone	DG B: 13, DG A: 5, DC B: 12, DC A: 4	C=C in quinazoline aromatic ring
Doxo-rubicin	−8.98	0.26 μM	DG B:13, DC A:4	Oxygen present in ester	DG B: 13, DC A: 4, DC B:12, DG A:5	C=C in amide aromatic ring

transforms into **3a** through a domino reaction sequence promoted by I_2/TBHP under optimized conditions.

Bioactivity studies

(i) Cytotoxicity assay. The synthesized derivatives were screened for their cytotoxicity towards cancer cell lines A549, B16-F10, DU145, and HepG2 and non-cancerous cell line CHO-K1 by MTT assay using doxorubicin as a standard drug. The cytotoxicity results expressed as IC_{50} values are depicted in Table 5.

Interestingly all the synthesized compounds exhibited significant cytotoxicity to cancer cell lines as compared to normal cell line. Predominantly, most of the compounds exhibited promising activity against DU145 and HepG2 cell lines. Notably, amongst all the derivatives, compounds **3o**, **3c** and **3l** displayed the most potent activity against DU145 and HepG2. From the structure–activity relationship perspective, it was seen that type of substitutions on quinazoline and amide pharmacophores affects the cytotoxic activity. Different substitutions on quinazoline ring like –Cl, –H, –F and –NO_2 showed activity in the order of Cl > H > F > NO_2. Whereas, substitutions on amide functionality like aromatic and aliphatic also influenced the cytotoxicity. Here, *N*-aryl functionality showed high activity as compared to *N*-alkyl functionality. Type of substitutions on aromatic ring also imparted effect on cytotoxicity which follows the order F > Br > Me > OMe. Compound **3o** having chlorine substitution on quinazoline pharmacophore with fluorine on aromatic ring of amide functionality displayed highly potent cytotoxicity. The compounds **3c** and **3l** are the next potent derivatives amongst the series. Here, **3c** has no substitution on quinazoline moiety and its amide functionality is substitution of *N*-(4-Me)Ph. In **3l**, fluorine substitution is present on quinazoline moiety and amide functionality is substituted with *N*-(4-Br)Ph. These observations suggest that presence of electron-withdrawing group on both the pharmacophores may be a promising factor for the high cytotoxicity.

(ii) Docking studies. Docking studies were implemented to validate the biological studies and to explore the plausible modes of interaction between the potent derivatives **3o**, **3c**, **3l** and DNA [Protein Data Bank (PDB) 1N37].[26] All the potent compounds were docked using AutoDock 4.2.6 against the promising anticancer target. For each ligand, the docking score was calculated in terms of kcal mol^{-1}. All the screened compounds, **3c**, **3l** and **3o** were found to interact with DG B:13, DG A:5, DC B:12 and DC A:4. The molecular docking results are tabulated in Table 6.

Binding interactions like hydrogen bond and π–π interactions, binding energies and inhibition constants of the molecules are used to explain the affinity of a molecule with DNA and stability of the complex. Fig. 2(A–C) depicts the binding interaction of **3c**, **3l**, and **3o** with DNA. From the figures it is clear that the molecules have been intercalated between the DNA base pairs. Docking studies showed that the compound **3c** exhibits strong H-bond interactions with higher binding energy (−9.13 kcal mol^{-1}) as compared to compounds **3l** (−8.31 kcal mol^{-1}) and **3o** (−8.04 kcal mol^{-1}).

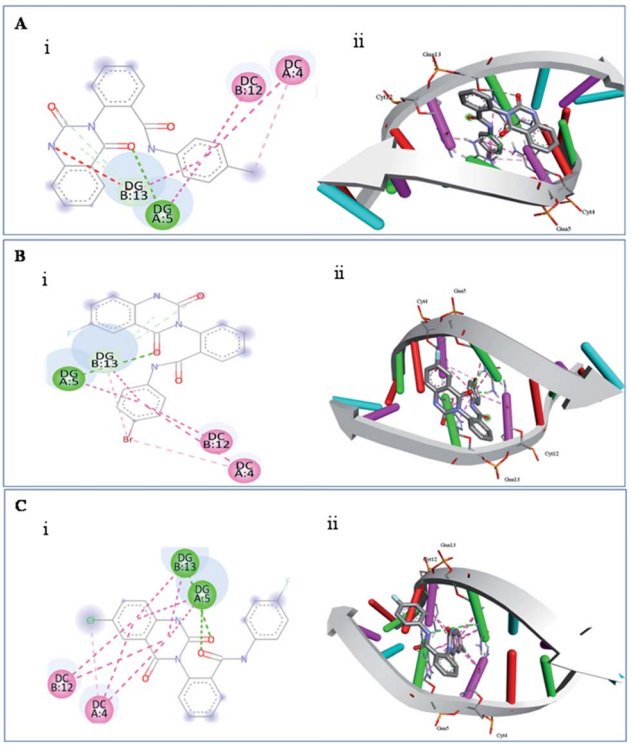

Fig. 2 Molecular docking (i) 2D and (ii) 3D binding interactions of (A) **3c**, (B) **3l** and (C) **3o** with the DNA (PDB 1N37); green lines correspond to hydrogen bonding and pink lines correspond to π–π stacking interactions with DNA.

Conclusions

We have developed a new and efficient metal-free oxidative domino reaction for preparation of 2-(2,4-dioxo-1,4-dihydro quinazolin-3(2*H*)-yl)-*N*-aryl/alkyl benzamides by reaction of an isatins with 2-amino *N*-aryl/alkyl benzamides using I_2/TBHP under mild conditions. These 2-(2,4-dioxo-1,4-dihydro quinazolin-3(2*H*)-yl)-*N*-aryl/alkyl benzamides consisted of quinazolines and amide moieties, which are important pharmacophores in several anticancer agents. In this study, the synthesized compounds also were found to display excellent cytotoxicity towards tested cancer cell lines A549, B16-F10, DU145, and HepG2 and no or lesser cytotoxic effects towards normal CHO-K1 cells. Especially, compounds **3c**, **3l** and **3o** exhibited promising bioactivity at micro molar concentration and these were found to be more potent than 5-flourouracil towards different cancer cell lines. Moreover, docking studies accomplished on these compounds also validated the results of cytotoxicity studies. The present study reveals that the compounds **3c**, **3l** and **3o** have potent therapeutic applications for treatment of different types of cancers.

Experimental section

General information

Melting points of all the compounds were recorded on Veego programmable melting point apparatus and are uncorrected. IR spectra were recorded on a PerkinElmer FT-IR 240-C spectrophotometer using KBr optics. ^{1}H NMR and ^{13}C NMR spectra were recorded on Bruker AV 400 MHz in $CDCl_3$ and DMSO-d_6 using TMS as internal standard. High resolution mass spectra (HRMS) [ESI$^+$] were obtained using either a TOF or a double focusing spectrometer, micro mass VG 70-70H or LC/MSD trap SL spectrometer operating at 70 eV using direct inlet system. All the reactions were monitored by thin layer chromatography (TLC) on percolated silica gel 60 F254 (mesh); spots were visualized with UV light. Merck silica gel (60–120 mesh) was used for column chromatography.

Typical procedure for synthesis of 2-(2,4-dioxo-1,2-dihydroquinazolin-3(4*H*)-yl)-*N*-phenylbenzamide (3a). Isatin **1a** (0.30 g, 2.04 mmol), 2-amino-*N*-phenylbenzamide **2a** (0.43 g, 2.04 mmol), iodine (0.15 g, 0.61 mmol), TBHP (0.56 ml, 70% aq, 4.08 mmol) and MeOH (10 mL) were taken into a round bottomed flask fitted with a condenser. The reaction mixture was stirred under reflux for 6 hours and progress of the reaction was monitored by TLC. Upon the completion of this reaction (monitored by TLC), the mixture was evaporated in vacuum, diluted with ethyl acetate (3 × 10 mL), and washed by hypo solution. The combined organic layer was washed with brine solution, dried over anhydrous Na_2SO_4 and concentrated under reduced pressure. The crude product was purified by normal column chromatography (silica gel 60–120 mesh, gradient solvent system of hexane–EtOAc) furnished 2-(2,4-dioxo-1,2-dihydroquinazolin-3(4*H*)-yl)-*N*-phenylbenzamide **3a** (0.62 g, 85%) as a white solid which gave satisfactory characterization data: mp: 274–276 °C.

^{1}H NMR (400 MHz, DMSO-d_6): δ 11.51 (1H, s), 10.37 (1H, s), 7.93–7.90 (1H, m), 7.82–7.80 (1H, m), 7.71–7.64 (2H, m), 7.60 (3H, d, J = 7.6 Hz), 7.47–7.45 (1H, m), 7.28–7.19 (4H, m), 7.05–7.01 (1H, m); ^{13}C NMR (100 MHz, DMSO-d_6): δ 163.69, 162.39, 150.26, 140.25, 140.21, 139.44, 137.52, 136.45, 135.81, 134.64, 133.31, 129.06, 128.12, 124.21, 123.09, 120.47, 115.78, 114.55, 94.96; FT-IR (KBr): ν 3281, 3220, 2951, 1715, 1660, 1439, 1321, 1268, 756 cm^{-1}; ESI-MS: m/z 358 [M + H]$^+$; ESI-HRMS: calcd for $C_{21}H_{16}N_3O_3$ [M + H]$^+$ 358.11862; found: 358.11995.

2-(2,4-dioxo-1,2-dihydroquinazolin-3(4*H*)-yl)-*N*-phenylbenzamide (3a). White solid; (yield: 85%), mp: 274–276 °C; ^{1}H NMR (400 MHz, DMSO-d_6): δ 11.51 (1H, s), 10.37 (1H, s), 7.93–7.90 (1H, m), 7.82–7.80 (1H, m), 7.71–7.64 (2H, m), 7.60 (3H, d, J = 7.6 Hz), 7.47–7.45 (1H, m), 7.28–7.19 (4H, m), 7.05–7.01 (1H, m); ^{13}C NMR (100 MHz, DMSO-d_6): δ 163.69, 162.39, 150.26, 140.25, 140.21, 139.44, 137.52, 136.45, 135.81, 134.64, 133.31, 129.06, 128.12, 124.21, 123.09, 120.47, 115.78, 114.55, 94.96; FT-IR (KBr): ν 3281, 3220, 2951, 1715, 1660, 1439, 1321, 1268, 756 cm^{-1}; ESI-MS: m/z 358 [M + H]$^+$; ESI-HRMS: calcd for $C_{21}H_{16}N_3O_3$ [M + H]$^+$ 358.11862; found: 358.11995.

2-(2,4-dioxo-1,2-dihydroquinazolin-3(4*H*)-yl)-*N*-(4-methoxy phenyl)benzamide (3b). Pale brown solid; (yield: 82%), mp: 255–257 °C; ^{1}H NMR (400 MHz, $CDCl_3$ + DMSO-d_6): δ 11.39 (1H, s), 9.99 (1H, s), 7.99 (1H, d, J = 7.9 Hz), 7.81 (1H, d, J = 7.3 Hz), 7.61–7.51 (5H, m), 7.37–7.35 (1H, m), 7.22 (1H, d, J = 8.1 Hz), 7.16 (1H, t, J = 7.5 Hz), 6.78–6.76 (2H, m), 3.75–3.71 (3H, m); ^{13}C NMR (100 MHz, $CDCl_3$ + DMSO-d_6): δ 169.65, 167.53, 160.67, 155.49, 144.88, 139.87, 139.82, 139.11, 137.18, 135.71, 135.24, 133.81, 133.27, 132.82, 127.36, 126.63, 120.44, 119.33, 118.54, 60.17; FT-IR (KBr): ν 3291, 3212, 2954, 1722, 1664, 1436, 1326, 1278, 759 cm^{-1}; ESI-MS: m/z 388 [M + H]$^+$; ESI-HRMS: calcd for $C_{22}H_{18}N_3O_4$ [M + H]$^+$ 388.12918; found: 388.13114.

2-(2,4-dioxo-1,2-dihydroquinazolin-3(4*H*)-yl)-*N*-(*p*-tolyl)benzamide (3c). White solid; (yield: 80%), mp: 245–247 °C; ^{1}H NMR (400 MHz, $CDCl_3$ + DMSO-d_6): δ 11.36 (1H, s), 9.84 (1H, s), 8.01 (1H, d, J = 7.9 Hz), 7.82 (1H, d, J = 7.5 Hz), 7.61–7.54 (3H, m), 7.49 (2H, d, J = 7.7 Hz), 7.36 (1H, d, J = 7.7 Hz), 7.21 (1H, d, J = 8.1 Hz), 7.16 (1H, t, J = 7.5 Hz), 7.03 (2H, d, J = 7.6 Hz), 5.40 (3H, s); ^{13}C NMR (100 MHz, $CDCl_3$ + DMSO-d_6): δ 169.80, 167.66, 155.59, 144.80, 141.30, 139.96, 139.84, 138.91, 138.31, 137.96, 135.80, 135.14, 133.88, 133.37, 132.86, 127.41, 125.03, 120.46, 119.28, 25.63; FT-IR (KBr): ν 3305, 3251, 2985, 1716, 1662, 1441, 1327, 1265, 753 cm^{-1}; ESI-MS: m/z 372 [M + H]$^+$; ESI-HRMS: calcd for $C_{22}H_{18}N_3O_3$ [M + H]$^+$ 372.13427; found: 372.13600.

2-(2,4-dioxo-1,2-dihydroquinazolin-3(4*H*)-yl)-*N*-(4-fluorophenyl) benzamide (3d). White solid; (yield: 70%), mp: 277–279 °C; ^{1}H NMR (400 MHz, $CDCl_3$ + DMSO-d_6): δ 11.40 (1H, s), 10.25 (1H, s), 7.99 (1H, d, J = 7.8 Hz), 7.82 (1H, d, J = 6.9 Hz), 7.62–7.55 (5H, m), 7.37 (1H, d, J = 7.5 Hz), 7.22 (1H, d, J = 8.0 Hz), 7.16 (1H, t, J = 7.4 Hz), 6.94 (2H, t, J = 8.4 Hz); ^{13}C NMR (100 MHz, $CDCl_3$ + DMSO-d_6): δ 169.90, 167.44, 164.67, 162.27, 155.39, 144.91, 140.40, 139.89, 139.54, 139.28, 135.89, 135.40, 133.82, 133.26, 132.80, 127.40, 126.76, 126.69, 120.46, 119.80, 119.32; FT-IR (KBr): ν 3291, 3226, 2965, 1721, 1663, 1436, 1315, 1260, 751 cm^{-1};ESI-MS: m/z 376 [M + H]$^+$; ESI-HRMS: calcd for $C_{21}H_{15}FN_3O_3$ [M + H]$^+$ 376.10920; found: 376.11086.

***N*-(4-Bromophenyl)-2-(2,4-dioxo-1,2-dihydroquinazolin-3(4*H*)-yl)benzamide (3e).** Wheatish solid; (yield: 78%), mp: 261–263 °C; ^{1}H NMR (400 MHz, $CDCl_3$ + DMSO-d_6): δ 11.43 (1H, s), 10.40 (1H, s), 7.97 (1H, d, J = 7.9 Hz), 7.81 (1H, d, J = 7.6 Hz), 7.65–7.53 (5H, m), 7.39–7.33 (3H, m), 7.22 (1H, d, J = 8.1 Hz), 7.17 (1H, t, J = 11.1 Hz); ^{13}C NMR (100 MHz, $CDCl_3$ + DMSO-d_6): δ 170.08, 167.53, 155.47, 144.85, 143.42, 139.91, 139.46, 139.22, 136.23, 136.04, 135.35, 133.86, 133.31, 132.84, 127.45, 126.73, 120.66, 120.49, 119.28; FT-IR (KBr): ν 3289, 3212, 2978, 1720, 1662, 1448, 1329, 1265, 752 cm^{-1}; ESI-MS: m/z 436 $[M + H]^+$; ESI-HRMS: calcd for $C_{21}H_{15}BrN_3O_3$ $[M + H]^+$ 436.02913; found: 436.03052.

2-(2,4-Dioxo-1,2-dihydroquinazolin-3(4*H*)-yl)-*N*-phenethyl benzamide (3f). White solid; (yield: 72%), mp: 207–209 °C; ^{1}H NMR (400 MHz, $CDCl_3$ + DMSO-d_6): δ 11.36 (1H, s), 8.00 (1H, d, J = 7.9 Hz), 7.82 (1H, s), 7.64–7.54 (3H, m), 7.48–7.45 (1H, m), 7.30 (1H, d, J = 7.8 Hz), 7.25–7.22 (3H, m), 7.17–7.15 (4H, m), 3.11 (2H, t, J = 9.8 Hz), 2.74 (2H, t, J = 7.1 Hz); ^{13}C NMR (100 MHz, $CDCl_3$ + DMSO-d_6): δ 171.33, 167.51, 155.48, 145.01, 144.36, 139.78, 139.58, 139.11, 135.54, 135.27, 133.60, 133.41, 133.26, 133.20, 132.73, 130.98, 127.30, 120.47, 119.41, 45.82, 40.16; FT-IR (KBr): ν 3285, 3215, 2976, 1718, 1664, 1436, 1326, 1265, 752 cm^{-1}; ESI-MS: m/z 386 $[M + H]^+$; ESI-HRMS: calcd for $C_{23}H_{20}N_3O_3$ $[M + H]^+$ 386.14992; found: 386.15168.

***N*-Butyl-5-chloro-2-(2,4-dioxo-1,2-dihydroquinazolin-3(4*H*)-yl)benzamide (3g).** Wheatish solid; (yield: 65%), mp: 203–205 °C; ^{1}H NMR (400 MHz, $CDCl_3$ + DMSO-d_6): δ 11.46 (1H, s), 8.18 (1H, s), 7.96 (1H, d, J = 7.5 Hz), 7.68 (1H, s), 7.61–7.53 (2H, m), 7.31 (1H, d, J = 8.1 Hz), 7.23 (1H, d, J = 8.0 Hz), 7.16 (1H, t, J = 7.4 Hz), 1.39 (1H, t, J = 6.7 Hz), 1.28–1.19 (4H, m), 0.81 (3H, t, J = 7.0 Hz); ^{13}C NMR (100 MHz, $CDCl_3$ + DMSO-d_6): δ 169.87, 167.37, 155.28, 144.97, 141.37, 139.92, 138.44, 137.77, 136.93, 135.25, 133.54, 132.71, 127.38, 120.50, 119.28, 43.98, 36.12, 24.68, 18.71; FT-IR (KBr): ν 3279, 3216, 2975, 1718, 1663, 1425, 1310, 1240, 761 cm^{-1}; ESI-MS: m/z 372 $[M + H]^+$; ESI-HRMS: calcd for $C_{19}H_{19}N_3O_3Cl$ $[M + H]^+$ 372.11095; found: 372.11240.

2-(2,4-Dioxo-1,2-dihydroquinazolin-3(4*H*)-yl)-*N*-ethyl-benzamide (3h). Pale brown solid; (yield: 75%), mp: 286–288 °C; ^{1}H NMR (400 MHz, $CDCl_3$ + DMSO-d_6): δ 11.40 (1H, s), 7.99 (1H, d, J = 7.8 Hz), 7.85 (1H, s), 7.68 (1H, d, J = 7.5 Hz), 7.61–7.54 (2H, m), 7.48 (1H, t, J = 7.5 Hz), 7.30 (1H, d, J = 7.7 Hz), 7.24 (1H, d, J = 8.2 Hz), 7.16 (1H, t, J = 7.6 Hz), 3.18 (2H, q, J = 13.2, 7.1 Hz), 1.04 (3H, t, J = 7.2 Hz); ^{13}C NMR (100 MHz, $CDCl_3$ + DMSO-d_6): δ 171.08, 167.44, 155.42, 145.01, 139.82, 139.73, 139.11, 135.42, 135.31, 133.37, 133.26, 132.70, 127.31, 120.43, 119.42, 39.04, 19.53; FT-IR (KBr): ν 3281, 3245, 2925, 1723, 1662, 1435, 1365, 1248, 748 cm^{-1}; ESI-MS: m/z 310 $[M + H]^+$; ESI-HRMS: calcd for $C_{17}H_{16}N_3O_3$ $[M + H]^+$ 310.11862; found: 310.11935.

2-(6-Fluoro-2,4-dioxo-1,2-dihydroquinazolin-3(4*H*)-yl)-*N*-phenyl benzamide (3i). Wheatish solid; (yield: 78%), mp: 160–162 °C; ^{1}H NMR (400 MHz, $CDCl_3$ + DMSO-d_6): δ 11.46 (1H, s), 10.13 (1H, s), 7.81 (1H, d, J = 10.0 Hz), 7.61–7.54 (5H, m), 7.39–7.31 (3H, m), 7.23 (3H, d, J = 5.9 Hz), 7.04–6.99 (1H, m); ^{13}C NMR (100 MHz, $CDCl_3$ + DMSO-d_6): δ 169.96, 166.77, 163.92, 161.52, 155.17, 144.09, 141.43, 139.62, 139.03, 135.90, 135.23, 133.94, 133.42, 128.58, 127.97, 127.73, 125.08, 122.60, 120.34, 120.26, 118.04, 117.80; FT-IR (KBr): ν 3279, 3215, 2987, 1721, 1661, 1438, 1325, 1265, 751 cm^{-1}; ESI-MS: m/z 376 $[M + H]^+$; ESI-HRMS: calcd for $C_{21}H_{15}FN_3O_3$ $[M + H]^+$ 376.10920; found: 376.11088.

2-(6-Fluoro-2,4-dioxo-1,2-dihydroquinazolin-3(4*H*)-yl)-*N*-(4-methoxyphenyl)benzamide (3j). Pale brown solid; (yield: 78%), mp: 160–162 °C; ^{1}H NMR (400 MHz, $CDCl_3$ + DMSO-d_6): δ 11.50 (1H, s), 10.05 (1H, s), 7.84 (3H, t, J = 8.8 Hz), 7.66–7.62 (2H, m), 7.57–7.51 (3H, m), 7.39–7.32 (2H, m), 7.28–7.22 (1H, m), 6.79 (2H, J = 8.9 Hz), 3.76 (3H, s); ^{13}C NMR (100 MHz, $CDCl_3$ + DMSO-d_6): δ 169.61, 166.80, 163.91, 161.51, 160.71, 155.20, 141.42, 139.70, 138.93, 137.10, 135.79, 135.15, 133.86, 133.40, 127.92, 127.68, 126.69, 122.57, 120.33, 118.55, 118.02, 117.78, 60.17; FT-IR (KBr): ν 3289, 3210, 2995, 1723, 1661, 1510, 1440, 1344, 1247, 752 cm^{-1}; ESI-MS: m/z 406 $[M + H]^+$; ESI-HRMS: calcd for $C_{22}H_{17}N_3O_4F$ $[M + H]^+$ 406.11976; found: 406.12108.

2-(6-Fluoro-2,4-dioxo-1,2-dihydroquinazolin-3(4*H*)-yl)-*N*-(4-fluorophenyl)benzamide (3k). Pale gray solid; (yield: 68%), mp: 262–264 °C; ^{1}H NMR (400 MHz, $CDCl_3$ + DMSO-d_6): δ 11.46 (1H, s), 10.20 (1H, s), 7.83 (1H, d, J = 7.3 Hz), 7.65–7.61 (4H, m), 7.55 (1H, t, J = 7.4 Hz), 7.38–732 (2H, m), 7.26–7.22 (1H, m), 6.94 (2H, t, J = 8.6 Hz); ^{13}C NMR (100 MHz, $CDCl_3$ + DMSO-d_6): δ 169.88, 166.81, 164.79, 163.94, 162.38, 161.54, 155.20, 141.40, 140.17, 139.47, 138.98, 135.96, 135.19, 133.89, 133.40, 127.94, 127.70, 126.79, 126.72, 122.58, 120.31, 120.00, 119.78, 118.05, 117.81; FT-IR (KBr): ν 3286, 3212, 2968, 1724, 1668, 1435, 1320, 1271, 753 cm^{-1}; ESI-MS: m/z 394 $[M + H]^+$; ESI-HRMS: calcd for $C_{21}H_{14}N_3O_3F_2$ $[M + H]^+$ 394.09977; found: 394.10152.

***N*-(4-Bromophenyl)-2-(6-fluoro-2,4-dioxo-1,2-dihydroquinazolin-3(4*H*)-yl)benzamide (3l).** Cream solid; (yield: 72%), mp: 272–274 °C; ^{1}H NMR (400 MHz, $CDCl_3$ + DMSO-d_6): δ 11.54 (1H, s), 10.45 (1H, s), 7.82 (1H, d, J = 6.5 Hz), 7.64–7.55 (5H, m), 7.38–7.35 (4H, m), 7.26 (1H, s); ^{13}C NMR (100 MHz, $CDCl_3$ + DMSO-d_6): δ 169.98, 166.60, 163.86, 161.46, 155.01, 143.60, 141.54, 139.24, 136.29, 136.11, 135.48, 133.89, 133.41, 128.16, 127.92, 126.83, 122.72, 122.64, 120.54, 120.33, 120.25, 117.93, 117.69; FT-IR (KBr): ν 3282, 3219, 2956, 1721, 1663, 1446, 1329, 1271, 758 cm^{-1}; ESI-MS: m/z 454 $[M + H]^+$; ESI-HRMS: calcd for $C_{21}H_{14}N_3O_3BrF$ $[M + H]^+$ 454.01971; found: 454.02096.

***N*-Ethyl-2-(6-fluoro-2,4-dioxo-1,2-dihydroquinazolin-3(4*H*)-yl)benzamide (3m).** Brown solid; (yield: 76%), mp: 225–227 °C; ^{1}H NMR: (400 MHz, $CDCl_3$ + DMSO-d_6): δ 11.21 (1H, s), 7.71–7.63 (2H, m), 7.55 (1H, d, J = 7.5 Hz), 7.48 (1H, t, J = 7.3 Hz), 7.29 (2H, t, J = 7.3 Hz), 7.22–7.18 (1H, m), 6.72 (1H, s), 3.28–3.25 (2H, m), 1.02 (3H, t, J = 6.9 Hz); ^{13}C NMR (100 MHz, $CDCl_3$ + DMSO-d_6): δ 171.16, 166.80, 163.89, 161.49, 155.23, 141.50, 139.64, 138.77, 135.51, 135.07, 133.42, 127.85, 127.61, 122.59, 122.52, 120.37, 120.29, 117.89, 117.65, 39.13, 19.46; FT-IR (KBr): ν 3275, 3205, 2916, 1716, 1675, 1435, 1358, 1271, 751 cm^{-1}; ESI-MS: m/z328 $[M + H]^+$; ESI-HRMS: calcd for$C_{17}H_{15}N_3O_3F$ $[M + H]^+$ 328.10147; found: 328.10210.

2-(6-Chloro-2,4-dioxo-1,2-dihydroquinazolin-3(4*H*)-yl)-*N*-phenylbenzamide (3n). White solid; (yield: 75%), mp: 165–167 °C; ^{1}H NMR (400 MHz, $CDCl_3$ + DMSO-d_6): δ 11.60 (1H, s), 10.28 (1H, s), 7.91 (1H, s), 7.83 (1H, s), 7.63–7.55 (5H, m), 7.40–7.34 (1H, m), 7.24–7.21 (3H, m), 7.01 (2H, d, J = 5.0 Hz); ^{13}C NMR (100 MHz, $CDCl_3$ + DMSO-d_6): δ 175.41, 169.93, 166.48, 155.12, 144.14, 143.60, 139.83, 139.55, 139.02, 135.91, 135.25,

133.97, 133.42, 132.29, 131.99, 128.57, 125.08, 122.40, 120.56; FT-IR (KBr): ν 3297, 3249, 3077, 1722, 1666, 1438, 1324, 1273, 754 cm^{-1}; ESI-MS: m/z 392 $[M + H]^+$; ESI-HRMS: calcd for $C_{21}H_{15}ClN_3O_3$ $[M + H]^+$ 392.07965; found: 392.08167.

2-(6-Chloro-2,4-dioxo-1,2-dihydroquinazolin-3(4*H*)-yl)-*N*-(4-fluorophenyl)benzamide (3o). Wheatish solid; (yield: 68%), mp: 265–267 °C; ^1H NMR (400 MHz, $CDCl_3$ + DMSO-d_6): δ 11.46 (1H, s), 10.00 (1H, s), 7.96 (1H, d, $J = 2.4$ Hz), 7.83 (1H, d, $J = 7.5$ Hz), 7.64–7.59 (3H, m), 7.55 (1H, d, $J = 7.4$ Hz), 7.51–7.48 (1H, m), 7.36 (1H, d, $J = 7.8$ Hz), 7.19 (1H, d, $J = 8.7$ Hz), 6.94 (2H, t, $J =$ 8.8 Hz); ^{13}C NMR (100 MHz, $CDCl_3$ + DMSO-d_6): δ 169.85, 166.62, 164.85, 162.44, 155.28, 143.48, 140.07, 139.79, 139.46, 138.86, 136.01, 135.13, 133.92, 133.46, 132.51, 132.12, 126.76, 126.69, 122.30, 120.48, 120.01, 119.79; FT-IR (KBr): ν 3302, 3240, 2922, 1731, 1661, 1503, 1370, 1224, 750 cm^{-1}; ESI-MS: m/z 410 $[M + H]^+$; ESI-HRMS: calcd for $C_{21}H_{14}N_3O_3ClF$ $[M + H]^+$ 410.07022; found: 410.07150.

2-(6-Chloro-2,4-dioxo-1,2-dihydroquinazolin-3(4*H*)-yl)-*N*-ethylbenzamide(3p). Pale brown solid; (yield: 74%), mp: 280–282 °C; ^1H NMR (400 MHz, $CDCl_3$ + DMSO-d_6): δ 11.37 (1H, s), 8.32 (1H, s), 8.00 (2H, s), 7.78 (1H, d, $J = 6.8$ Hz), 7.66 (1H, d, $J =$ 7.6 Hz), 7.30 (1H, d, $J = 7.6$ Hz), 7.20 (1H, d, $J = 8.6$ Hz), 6.68 (1H, s), 3.27 (2H, q, $J = 12.8$, 6.0 Hz), 1.05 (3H, t, $J = 7.3$ Hz); ^{13}C NMR (100 MHz, $CDCl_3$ + DMSO-d_6): δ 171.02, 166.45, 155.13, 143.71, 139.74, 139.47, 138.88, 135.50, 135.19, 133.45, 133.38, 132.09, 131.82, 122.42, 120.64, 39.08, 19.52; FT-IR (KBr): ν 3301, 3245, 2941, 1726, 1665, 1462, 1352, 1245, 753 cm^{-1}; ESI-MS: m/z 344 $[M + H]^+$; ESI-HRMS: calcd for $C_{17}H_{15}N_3O_3Cl$ $[M + H]^+$ 344.07965; found: 344.07831.

***N*-Butyl-5-chloro-2-(6-chloro-2,4-dioxo-1,2-dihydroquinazolin-3(4*H*)-yl)benzamide (3q).** Pale brown solid; (yield: 72%), mp: 205–207 °C; ^1H NMR (400 MHz, $CDCl_3$ + DMSO-d_6): δ 11.59 (1H, s), 8.03 (1H, s), 7.93–7.92 (1H, m), 7.70 (1H, s), 7.54–7.52 (2H, m), 7.29–7.26 (1H, m), 7.23 (1H, d, $J = 8.7$ Hz), 1.41 (2H, t, $J = 6.7$ Hz), 1.31–1.22 (4H, m), 0.85–0.81 (3H, t, J = 7.3 Hz); ^{13}C NMR (100 MHz, $CDCl_3$ + DMSO-d_6): δ 169.92, 166.48, 155.05, 143.58, 141.16, 139.85, 138.78, 137.30, 136.63, 135.37, 133.62, 132.36, 131.90, 122.44, 120.42, 44.08, 36.11, 24.69, 18.65; FT-IR(KBr): ν 3292, 3216, 2997, 1723, 1665, 1436, 1329, 1245, 750 cm^{-1}; ESI-MS: m/z 406 $[M + H]^+$; ESI-HRMS: calcd for $C_{19}H_{18}N_3O_3Cl_2$ $[M + H]^+$ 406.07197; found: 406.07371.

2-(6-Nitro-2,4-dioxo-1,2-dihydroquinazolin-3(4*H*)-yl)-*N*-phenylbenzamide (3r). Pale yellow solid; (yield: 68%), mp: 195–198 °C; ^1H NMR (400 MHz, $CDCl_3$ + DMSO-d_6): δ 12.13 (1H, s), 10.33 (1H, s), 8.79–8.77 (1H, m), 8.41 (1H, d, $J = 8.9$ Hz), 7.87 (1H, d, $J = 7.3$ Hz), 7.68–7.57 (4H, m), 7.42–7.39 (2H, m), 7.23 (2H, t, $J = 7.6$ Hz), 7.02 (1H, t, $J = 7.1$ Hz); ^{13}C NMR (100 MHz, $CDCl_3$ + DMSO-d_6): δ 169.82, 166.10, 154.94, 149.58, 147.32, 144.06, 139.19, 138.65, 136.11, 135.22, 134.50, 134.10, 133.68, 133.44, 129.36, 128.65, 125.16, 121.84, 119.30; FT-IR (KBr): ν 3285, 3234, 2960, 1718, 1663, 1446, 1322, 1261, 751 cm^{-1}; ESI-MS: m/z 403 $[M + H]^+$; ESI-HRMS: calcd for $C_{21}H_{15}N_4O_5$ $[M + H]^+$ 403.10370; found: 403.10511.

2-(2,4-Dioxo-1,4-dihydroquinazolin-3(2*H*)-yl)-5-methoxy-*N*-phenylbenzamide (3s). Brown solid; (yield: 81%), mp: 234–236 °C; ^1H NMR (400 MHz, $CDCl_3$ + DMSO-d_6): δ 11.03 (1H, s), 9.38 (1H, s), 7.71 (2H, d, $J = 7.3$ Hz), 7.51 (2H, d, J 7.4 Hz), 7.33–7.21 (5H, m), 7.05 (2H, t, $J = 7.9$ Hz), 6.92 (1H, t, $J = 8.5$ Hz), 6.86 (1H, d, $J = 7.7$ Hz), 6.48 (2H, t, $J = 8.5$ Hz), 3.44 (3H, s); ^{13}C NMR (100 MHz, $CDCl_3$ + DMSO-d_6): δ 163.71, 161.63, 154.73, 149.59, 138.91, 133.98, 133.85, 133.10, 131.19, 129.77, 129.25, 127.87, 127.34, 126.89, 121.41, 120.66, 114.49, 113.38, 112.59, 54.22; FT-IR (KBr): ν 3273, 3214, 2936, 1719, 1659, 1439, 1321, 1271, 753 cm^{-1}; ESI-MS: m/z 388 $[M + H]^+$; ESI-HRMS: calcd for $C_{22}H_{18}N_3O_4$ $[M + H]^+$ 388.12918; found: 388.12973.

5-Chloro-2-(2,4-dioxo-1,4-dihydroquinazolin-3(2*H*)-yl)-*N*-phenylbenzamide (3t). Wheatish solid; (yield: 71%), mp: 245–247 °C; ^1H NMR (400 MHz, $CDCl_3$ + DMSO-d_6): δ 11.83 (1H, s), 10.54 (1H, s), 8.08 (1H, s), 8.03 (1H, d, $J = 6.8$ Hz), 7.83–7.77 (5H, m), 7.59 (1H, s), 7.43 (3H, s), 7.22 (1H, d, $J = 6.8$ Hz); ^{13}C NMR (100 MHz, $CDCl_3$ + DMSO-d_6): δ 164.95, 161.58, 150.23, 139.05, 138.56, 134.82, 134.63, 133.93, 130.95, 130.18, 128.99, 128.44, 127.43, 127.10, 123.61, 120.09, 117.37, 115.55; FT-IR (KBr): ν 3280, 3229, 2985, 1716, 1653, 1432, 1312, 1260, 752 cm^{-1}; ESI-MS: m/z 392 $[M + H]^+$; ESI-HRMS: calcd for $C_{21}H_{15}ClN_3O_3$ $[M + H]^+$ 392.07965; found: 392.07895.

2-(2,4-Dioxo-1,4-dihydroquinazolin-3(2*H*)-yl)-5-nitro-*N*-phenylbenzamide (3u). Pale yellow solid; (yield: 60%), mp: 228–230 °C; ^1H NMR (400 MHz, $CDCl_3$ + DMSO-d_6): δ 11.69 (1H, s), 9.74 (1H, s), 8.47 (1H, d, $J = 2.2$ Hz), 8.00 (1H, d, J 6.5 Hz), 7.50 (1H, d, $J = 7.5$ Hz), 7.28–7.22 (4H, m), 7.02–7.00 (2H, m), 6.86 (2H, t, $J = 7.9$ Hz), 6.65 (1H, t, $J = 7.4$ Hz); ^{13}C NMR (100 MHz, $CDCl_3$ + DMSO-d_6): δ 164.10, 160.42, 149.33, 143.80, 141.63, 138.14, 133.58, 132.74, 130.36, 129.29, 128.57, 128.38, 127.96, 127.69, 123.89, 122.94, 119.39, 116.01, 113.57; FT-IR (KBr): ν 3275, 3214, 2968, 1721, 1652, 1441, 1345, 1215, 758 cm^{-1}; ESI-MS: m/z 403 $[M + H]^+$; ESI-HRMS: calcd for $C_{21}H_{15}N_4O_5$ $[M + H]^+$ 403.10370; found: 403.10461.

5*H*-Quinazolino[3,2-*a*]quinazoline-5,12(7*H*)-dione (6a). Brown solid; (yield: 82%), mp: 236–238 °C; ^1H NMR (400 MHz, $CDCl_3$ + DMSO-d_6): δ 8.61–8.49 (1H, m), 8.32–8.24 (1H, m), 8.02 (1H, s), 7.81–7.76 (1H, m), 7.73–7.69 (1H, m), 7.55 (1H, d, $J = 8.5$ Hz), 7.51–7.48 (1H, m), 7.31–7.13 (2H, m); ^{13}C NMR (100 MHz, $CDCl_3$ + DMSO-d_6): δ163.39, 161.70, 160.27, 148.65, 144.56, 137.19, 135.03, 134.14, 133.59, 127.38, 126.97, 126.72, 126.10, 123.25, 115.16; FT-IR (KBr): ν 3254, 3011, 1719, 1642, 1451, 1332, 1265, 757 cm^{-1}; ESI-MS: m/z 264 $[M + H]^+$; ESI-HRMS: calcd for $C_{15}H_{10}N_3O_2$ $[M + H]^+$ 264.07675; found: 264.07608.

10-Chloro-5*H*-quinazolino[3,2-*a*]quinazoline-5,12(7*H*)-dione (6b). Wheatish solid; (yield: 79%), mp: 182–185 °C; ^1H NMR (400 MHz, $CDCl_3$ + DMSO-d_6): δ 8.55 (1H, d, $J = 3.4$ Hz), 8.24 (1H, s), 8.00 (2H, d, $J = 3.0$ Hz), 7.78–7.75 (1H, m), 7.71–7.68 (1H, m), 7.50–7.47 (2H, m); ^{13}C NMR (100 MHz, $CDCl_3$ + DMSO-d_6): δ 167.27, 166.56, 165.15, 153.57, 150.08, 149.46, 147.59, 139.79, 139.02, 134.11, 132.09, 131.61, 130.97, 127.76, 122.20; FT-IR (KBr): ν 3256, 3021, 1722, 1645, 1432, 1341, 1236, 751 cm^{-1}; ESI-MS: m/z 298 $[M + H]^+$; ESI-HRMS: calcd for $C_{15}H_9N_3O_2Cl$ $[M + H]^+$ 298.03125; found: 298.03194.

Typical procedure for synthesis of (*Z*)-2-((2-oxoindolin-3-ylidene)amino)-*N*-phenylbenzamide (4a). Isatin **1a** (0.30 g, 2.04 mmol), 2-amino-*N*-phenylbenzamide **2a** (0.43 g, 2.04 mmol), iodine (0.15 g, 0.61 mmol) and MeOH (10 mL) were taken into a round bottomed flask fitted with a condenser. The reaction mixture was stirred under reflux for 2 hours and progress of the

reaction was monitored by TLC. Upon the completion of this reaction (monitored by TLC), the mixture was evaporated in vacuum, diluted with ethyl acetate (3 × 10 mL), and washed by hypo solution. The combined organic layer was washed with brine solution, dried over anhydrous Na_2SO_4 and concentrated under reduced pressure. The crude product was purified by normal column chromatography (silica gel 60–120 mesh, gradient solvent system of hexane–EtOAc) furnished (*Z*)-2-((2-oxoindolin-3-ylidene) amino)-*N*-phenylbenzamide **4a** (0.63 g, 90%)as a pale brown solid which gave satisfactory characterization data.

(*Z*)-2-((2-Oxoindolin-3-ylidene)amino)-*N*-phenyl benzamide (4a). Pale brown solid (Yield: 90%), mp: 225–227 °C; ^{1}H NMR (400 MHz, DMSO-d_6): δ 11.54 (1H, s), 10.45 (1H, s), 8.12 (1H, d, J = 1.6 Hz), 8.04–8.01 (1H, m Hz), 7.91 (1H, d, J = 7.2 Hz), 7.69 (1H, t, J = 7.0 Hz), 7.58 (2H, d, J = 7.8 Hz), 7.29–7.25 (3H, m), 7.20 (2H, d, J = 7.8 Hz), 7.04 (1H, t, J = 7.4 Hz); ^{13}C NMR (100 MHz, DMSO-d_6): δ 163.69, 162.39, 150.26, 140.25, 140.21, 139.44, 137.52, 136.45, 135.81, 134.64, 133.31,129.06, 128.12, 124.21, 123.09, 120.47, 115.78, 114.55, 94.96; FT-IR (KBr): ν 3212, 3150, 2920, 1718, 1656, 1428, 1325, 1259, 752 cm^{-1}; ESI-MS: m/z 342 [M + H]$^+$; ESI-HRMS: calcd for $C_{21}H_{16}N_3O_2$ [M + H]$^+$ 342.12370; found: 342.12497.

Typical procedure for synthesis of (*Z*)-2-((2-oxo-1*H*-benzo[*d*][1,3]oxazin-4(2*H*)-ylidene)amino)-*N*-phenyl benzamide (5a). (*Z*)-2-((2-Oxoindolin-3-ylidene)amino)-*N*-phenyl benzamide **4a** (0.5 g, 1.46 mmol) and MeOH (10 mL) were taken into a round bottomed flask fitted with a condenser. Then add 70% TBHP (0.4 ml, 2.93 mmol) to reaction mixture was stirred under reflux for 2 hours and progress of the reaction was monitored by TLC. Upon the completion of this reaction (monitored by TLC), the mixture was evaporated in vacuum, diluted with ethyl acetate (3 × 10 mL). The combined organic layer was washed with brine solution, dried over anhydrous Na_2SO_4 and concentrated under reduced pressure. The crude product was purified by normal column chromatography (silica gel 60–120 mesh, gradient solvent system of hexane–EtOAc) furnished typical procedure for synthesis of (*Z*)-2-((2-oxo-1*H*-benzo[*d*][1,3] oxazin-4(2*H*)-ylidene)amino)-*N*-phenylbenzamide **5a** (0.49 g, 95%) as a pale brown solid which gave satisfactory characterization data.

(*Z*)-2-((2-Oxo-1*H*-benzo[*d*][1,3]oxazin-4(2*H*)-ylidene)amino)-*N*-phenylbenzamide (5a). Pale brown; (yield: 95%), mp: 246–248 °C; ^{1}H NMR (400 MHz, $CDCl_3$): δ 9.63 (1H, s), 8.34 (1H, s), 8.00 (1H, d, J = 7.8 Hz), 7.69 (1H, d, J = 6.1 Hz), 7.45–7.37 (5H, m), 7.22 (1H, d, J = 7.2 Hz), 7.14 (2H, t, J = 7.6 Hz), 7.08 (1H, d, J = 7.4 Hz), 6.96 (1H, t, J = 7.2 Hz), 6.84 (1H, d, J = 7.0 Hz); ^{13}C NMR (100 MHz, $CDCl_3$ + DMSO-d_6): δ 165.05, 163.02, 150.92, 139.85, 138.73, 135.31, 135.01, 133.68, 131.15, 130.17, 129.02, 128.71, 128.62, 128.14, 123.81, 122.65, 119.98, 115.62, 114.41; FT-IR (KBr): ν 3244, 3070, 2940, 1716, 1642, 1451, 1321, 1272, 759 cm^{-1}; ESI-MS: m/z 358 [M + H]$^+$; ESI-HRMS: calcd for $C_{21}H_{16}N_3O_3$ [M + H]$^+$ 358.11862; found: 358.11718.

MTT assay

All the synthesized compounds were tested for their cytotoxicity efficacy using MTT assay on both cancer and normal cell lines following the protocol of our earlier published literature.[27]

For this assay, cancer lines A549 – *Homo sapiens* lung carcinoma (ATCC® CCL-185™); B16-F10 – *Mus musculus* mouse skin melanoma (ATCC® CRL 6475™); DU145 – *Homo sapiens* prostrate carcinoma (ATCC® HTB-81™); Hep G2 – *Homo sapiens* hepatocellular carcinoma (ATCC® HB-8065™); CHO-K1 – *Cricetulus griseus* Chinese hamster ovary cells (ATCC® CCL-61™) were used. All the cell lines used in this study were obtained from the ATCC (Bethesda, MD, USA) and grown in DMEM with 10% Fetal Bovine (FBS) along with 100 U mL^{-1} penicillin, 100 μg mL^{-1} streptomycin and 2 mM L-glutamine. Initially, each cell line was grown in the 96 well culture plate at 37 °C at 5% CO_2 in an incubator and allowed to attach properly. After attaining the growth of cells, each test compound at different concentrations (from 1 to 100 μM) was treated to the cells and incubated for 24 h. After the incubation of the cells, MTT (0.5 mg mL^{-1}) was added and further incubated for 3 h. About 100 μl DMSO was added to each well to dissolve the insoluble formazan crystals and finally, the absorbance reading was taken for each plate using a multi-mode plate reader, all the experiments were carried out in triplicate and 50% inhibitory concentration (IC_{50} value) of each compound was calculated using Graphpad prism-6. Simultaneously, 5-fluorouracil (**5FU**) and doxorubicin were used as positive control and standard drug respectively for the comparison of cytotoxicity activity of the test compounds.

Molecular docking

In order to explore plausible interaction models of compounds **3c**, **3l** and **3o**, docking studies were performed with the anti-parallel propeller type telomeric DNA and oncogene c-Myc promoter [Protein Data Bank (PDB) entry 1N37].[26] The protein and ligand preparation were performed using Discovery studio 2021.[28] Molecular docking was carried out using AutoDock 4.2.6 version.[29] The structures of **3c**, **3l** and **3o** were drawn and converted into 3D molecules using Discovery studio 2021. Water molecules were eliminated and the polar hydrogen atoms were added to the PDB system. To check the interactions of the ligands with all G-quadruplex DNA conformations, a docking experiment was done on the active site using AutoDock tools-1.5.7 and the best docked structure was taken using a dG-score (G score) function. The DNA–ligand interactions were visualized and the 3D & 2D figures were generated using the Discovery studio 2021. The protein–ligand interactions as *g*-score are tabulated in Table 6.

Conflicts of interest

The authors declare that they have no conflict of interest.

Acknowledgements

Authors A. K. S., and V. K. E. are thankful to UGC, New Delhi S. K. C. is thankful to CSIR, New Delhi for financial support in the form of research fellowship. I am thankful to DKIM Division (IICT Communication No. IICT/Pubs./2022/094) for the support.

Notes and references

1 (*a*) N. Kerru, P. Singh, N. Koorbanally, R. Raj and V. Kumar, *Eur. J. Med. Chem.*, 2017, **142**, 179; (*b*) A. Ouahrouch, H. Ighachane, M. Taourirte, J. W. Engels, M. H. Sedra and H. B. Lazrek, *Arch. Pharm. Chem. Life Sci.*, 2014, **347**, 1; (*c*) P. S. Auti, G. George and A. T. Paul, *RSC Adv.*, 2020, **10**, 41353; (*d*) P. S. Singu, U. Chilakamarthi, N. S. Mahadik, B. Keerti, N. Valipenta, S. N. Mokale, N. Nagesh and R. M. Kumbhare, *RSC Med. Chem.*, 2021, **12**, 416.

2 N. Kerru, L. Gummidi, S. Maddila, K. K. Gangu and S. B. Jonnalagadda, *Molecules*, 2020, **25**, 1909.

3 E. F. Ismail, I. A. I. Ali, W. Fathalla, A. A. Alsheikh and E. S. E. Tamney, *Arkivoc*, 2017, 104.

4 A. A. El-Barbary, A. A. El-Shehawy and N. I. Abdo, *Phosphorus, Sulfur Silicon Relat. Elem.*, 2014, **183**, 400.

5 I. M. El-Deeb, S. M. Bayoumi, M. A. El-Sherbeny and A. A.-M. Abdel-Aziz, *Eur. J. Med. Chem.*, 2010, **45**, 2516.

6 (*a*) S. I. Mirallai, M. J. Manos and P. A. Koutentis, *J. Org. Chem.*, 2013, **78**, 9906; (*b*) E. Enciso, J. Sarmiento-Sanchez, H. S. Lopez-Moreno, A. Ochoa-Teran, U. Osuna-Martinez and E. Beltran-Lopez, *Mol. Diversity*, 2016, **20**, 821; (*c*) I. A. Rivero, K. Espinoza and R. Somanathan, *Molecules*, 2004, **9**, 609.

7 D. Kang, H. Zhang, Z. Zhou, B. Huang, L. Naesens, P. Zhan and X. Liu, *Bioorg. Med. Chem. Lett.*, 2016, **26**, 5182.

8 A. H. Abdelmonsef and A. M. Mosallam, *J. Heterocycl. Chem.*, 2020, **1**, 1–18.

9 A. N. Al-Romaizan, N. S. Ahmed and S. M. Elfeky, *Journal of Chemistry*, 2019, **1**, 1–12.

10 M. Redondo, J. G. Zarruk, P. Ceballos, D. I. Perez, C. Perez, A. Perez-Castillo, M. A. Moro, J. Brea, C. Val, M. I. Cadavid, M. I. Loza, N. E. Campillo, A. Martinez and C. Gil, *Eur. J. Med. Chem.*, 2012, **47**, 175.

11 A. Nakagawa, S. Uno, M. Makishima, H. Miyachi and Y. Hashimoto, *Bioorg. Med. Chem.*, 2008, **16**, 7046.

12 T. P. Tran, E. L. Ellsworth, M. A. Stier, J. M. Domagala, H. D. H. Showalter, S. J. Gracheck, M. A. Shapiro, T. E. Joannides and R. Singh, *Bioorg. Med. Chem. Lett.*, 2004, **14**, 4405.

13 H. Kakuta, A. Tanatani, K. Nagasawa and Y. Hashimoto, *Chem. Pharm. Bull.*, 2003, **51**, 1273.

14 S. H. Watterson, G. V. D. Lucca, Q. Shi, C. M. Langevine, Q. Liu, D. G. Batt, M. B. Bertrand, H. Gong, J. Dai, S. Yip, P. Li, D. Sun, D.-R. Wu, C. Wang, Y. Zhang, S. C. Traeger, M. A. Pattoli, S. Skala, L. Cheng, M. T. Obermeier, R. Vickery, L. N. Discenza, C. J. Darienzo, Y. Zhang, E. Heimrich, K. M. Gillooly, T. L. Taylor, C. Pulicicchio, K. W. Mcintyre, M. A. Galella, A. J. Tebben, J. K. Muckelbauer, C. Y. Chang, R. Rampulla, A. Mathur, L. Salter-Cid, J. C. Barrish, P. H. Carter, A. Fura, J. R. Burke and J. A. Tino, *J. Med. Chem.*, 2016, **59**, 9173.

15 (*a*) M. Demeunynck and I. Baussanne, *Curr. Med. Chem.*, 2013, **20**, 794; (*b*) M. Asif, *Int. J. Med. Biochem.*, 2014, 395637.

16 N. F. Lazareva and V. F. Sidorkin, *Efficient Methods for Preparing Silicon Compounds*, 2016, p. 295.

17 P. Rajput and A. Sharma, *Journal of Pharmacology and Medicinal Chemistry*, 2018, **2**, 22.

18 (*a*) P. S. Singu, S. Kanugala, S. A. Dhawale, C. G. Kumar and R. M. Kumbhare, *ChemistrySelect*, 2020, **5**, 117; (*b*) K. Chavva, S. Pillalamarri, V. Banda, S. Gautham, J. Gaddamedi, P. Yedla, C. G. Kumar and N. Banda, *Bioorg. Med. Chem. Lett.*, 2013, **23**, 5893; (*c*) G. J. Dev, Y. Poornachandra, K. R. Reddy, R. N. Kumar, N. Ravikumar, D. K. Swaroop, P. Ranjitreddy, G. S. Kumar, J. B. Nanubolu, C. G. Kumar and B. Narsaiah, *Eur. J. Med. Chem.*, 2017, **130**, 223; (*d*) N. R. Kumar, D. K. Swaroop, N. Punna, K. Sirisha, T. Ganapathi, C. G. Kumar and B. Narsaiah, *ChemistrySelect*, 2018, **3**, 7813.

19 J. Boonen, A. Bronselaer, J. Nielandt, L. Veryser, G. D. Tre and B. D. Spiegeleer, *J. Ethnopharmacol.*, 2012, **142**, 563.

20 A. Harrington and Y. Tal-Gan, *Future Med. Chem.*, 2019, **11**, 2759.

21 (*a*) E. Spaczynska, A. Mrozek-Wilczkiewicz, K. Malarz, J. Kos, T. Gonec, M. Oravec, R. Gawecki, A. Bak, J. Dohanosova, I. Kapustikova, T. Liptaj, J. Jampilek and R. Musiol, *Sci. Rep.*, 2019, **9**, 6387; (*b*) N. S. Thirukovela, S. K. Nukala, N. Sirassu, R. Manchal, P. Gundepaka and S. Paidakula, *ChemistrySelect*, 2020, **5**, 12317; (*c*) Z.-H. Zhang, H.-M. Wu, S.-N. Deng, X.-Y. Cai, Y. Yao, M. C. Mwenda, J.-Y. Wang, D. Cai and Y. Chen, *Journal of Chemistry*, 2018, **1**, 1–8.

22 (*a*) X. Zhou, X. Xie and G. Liu, *Mol. Diversity*, 2013, **17**, 197; (*b*) J. Zhou, M. Ji, H. Yao, R. Cao, H. Zhao, X. Wang, X. Chen and B. Xu, *Org. Biomol. Chem.*, 2018, **1**, 1–17.

23 (*a*) M. C. Willis, R. H. Snell, A. J. Fletcher and R. L. Woodward, *Org. Lett.*, 2006, **8**, 5089; (*b*) C. Larksarp and H. Alper, *J. Org. Chem.*, 2000, **65**, 2773; (*c*) X. Wu and Z. Yu, *Tetrahedron Lett.*, 2010, **51**, 1500; (*d*) H. Chen, P. Li, R. Qin, H. Yan, G. Li and H. Huang, *ACS Omega*, 2020, **5**, 9614; (*e*) G. Shi, X. He, Y. Shang, C. Yang and L. Xiang, *Chin. J. Chem.*, 2017, 1; (*f*) D.-Q. Shi, G.-L. Dou, Z.-Y. Li, S.-N. Ni, X.-Y. Li, X.-S. Wang, H. Wu and S.-J. Ji, *Tetrahedron*, 2007, **63**, 9764.

24 (*a*) H.-X. Wang, T.-Q. Wei, P. Xu, S.-Y. Wang and S.-J. Ji, *J. Org. Chem.*, 2018, **83**, 13491; (*b*) G. C. Senadi, W.-P. Hu, T.-Y. Lu, A. M. Garkhedkar, J. K. Vandavasi and J.-J. Wang, *Org. Lett.*, 2015, **17**, 1521; (*c*) Y. Zi, Z.-J. Cai, S.-Y. Wang and S.-J. Ji, *Org. Lett.*, 2014, **16**, 3094.

25 (*a*) A. Nagaraju, B. J. Ramulu, G. Shukla, A. Srivastav, G. K. Verma, K. Raghuvanshi and M. S. Singh, *Green Chem.*, 2015, **17**, 950–958; (*b*) Y.-W. Sun and L.-Z. Wang, *New J. Chem.*, 2018, **42**, 20032–20040; (*c*) S. Muthusaravanan, B. D. Bala and S. Perumal, *Tetrahedron Lett.*, 2013, **54**, 5302–5306; (*d*) S. Su, J. Li, M. Sun, H. Zhao, Y. Chen and J. Li, *Chem. Commun.*, 2018, **54**, 9611–9614; (*e*) B. Jiang, G. Zhang, N. Ma, F. Shi, S.-J. Tu, P. Kaur and G. Li, *Org. Biomol. Chem.*, 2011, **9**, 3834–3838.

26 M. S. Searle, A. J. Maynard and H. E. L. Williams, *Org. Biomol. Chem.*, 2003, **1**, 60.

27 M. Balakrishna, M. S. L. Karuna, R. B. N. Prasad, E. V. Krisha, S. Misra, C. G. Kumar and S. S. Kaki, *SN Appl. Sci.*, 2020, **2**, 1229.

28 *BIOVIA Discovery studio visualizer*, San Diego, Dassault Systemes, 2021.

29 G. M. Morris, D. S. Goodsell, M. E. Pique, W. L. Lindstrom, R. Huey, S. Forli, W. E. Hart, S. Halliday, R. Belew and A. J. Olson, *Automated Docking*, 2014.